

ORDER, DISORDER, AND PHASE TRANSITION  
IN CONDENSED SYSTEM

## Role of Superexchange Interactions in the Ferromagnetism of Manganites

I. O. Troyanchuk<sup>a\*</sup>, M. V. Bushinsky<sup>a</sup>, N. V. Volkov<sup>b</sup>, V. Sikolenko<sup>c</sup>, E. A. Efimova<sup>d</sup>, and C. Ritter<sup>e</sup>

<sup>a</sup> Scientific and Practical Materials Research Centre, National Academy of Sciences of Belarus,  
ul. P. Brovki 19, Minsk, 220072 Belarus

\*e-mail: troyan@physics.by

<sup>b</sup> Kirensky Institute of Physics, Siberian Branch, Russian Academy of Sciences, Akademgorodok, Krasnoyarsk, 660036 Russia

<sup>c</sup> Helmholtz Center Berlin, Lise-Meitner-Pl. 1, Berlin, 14109 Germany

<sup>d</sup> Joint Institute for Nuclear Research, Dubna, Moscow oblast, 141980 Russia

<sup>e</sup> Institut Laue–Langevin, Grenoble Cedex 9, 38042 France

Received May 5, 2014

**Abstract**—Compound  $\text{La}_{0.7}\text{Sr}_{0.3}\text{Mn}_{0.85}\text{Nb}_{0.15}\text{O}_3$ , in which manganese ions are in an oxidation state close to  $3+$ , are studied by neutron diffraction and magnetic measurements. This compound is shown to be a ferromagnet with  $T_C = 145$  K and a magnetic moment of  $3.1 \mu_B/\text{Mn}$  at  $T = 10$  K. No signs of cooperative orbital ordering are detected. When  $\text{Mg}^{2+}$  ions substitute for some  $\text{Nb}^{5+}$  ions,  $\text{Mn}^{4+}$  ions appear but ferromagnetism is not enhanced. An increase in the structural distortions leads to a decrease in the ferromagnetic component. The ferromagnetic state is assumed to be caused by substantial hybridization of the  $e_g$  orbitals of manganese and oxygen, which increases the positive part of the superexchange interactions.

DOI: 10.1134/S1063776115010173

### 1. INTRODUCTION

The ferromagnetism of  $\text{Ln}_{1-x}\text{A}_x\text{MnO}_3$  (Ln is a lanthanide, A is an alkaline-earth ion) is usually explained in terms of the double exchange model proposed by Zener in 1951 [1]. In this model, the ferromagnetism is caused by the free motion of charge carriers between manganese ions having different valences. It is assumed that the superexchange interactions here are mainly antiferromagnetic and weakly contribute to the ferromagnetic part of exchange [2]. The competition between ferromagnetic and antiferromagnetic interactions can cause colossal magnetoresistance [2].

De Gennes [3] developed the double exchange theory and predicted the appearance of a noncollinear magnetic structure during the concentration transition of the antiferromagnetic state ( $\text{LnMnO}_3$ ) into the ferromagnetic state ( $\text{Ln}_{1-x}\text{A}_x\text{MnO}_3$ ,  $x = 0.2$ ). However, NMR [4, 5] and neutron diffraction [6, 7] studies count in favor of the formation of a mixed two-phase magnetic state. Moreover, it was found that a ferromagnetic state can appear in manganites without the effect of mixed valence of  $\text{Mn}^{3+}$  and  $\text{Mn}^{4+}$  ions [8–13]. For example, above the orbital order–disorder transition temperature (near 750 K), the base compound  $\text{LaMnO}_3$  behaves like a ferromagnet (with regard to magnetic properties) with an approximated Curie point of 160 K [12]. This means that orbital disordering leads to the transition from antiferromagnetic to ferromagnetic exchange interactions. A long-

range ferromagnetic order was found to appear in the  $\text{LaMn}_{1-x}\text{Ga}_x\text{O}_3$  system at  $x > 0.15$  without  $\text{Mn}^{4+}$  ions [8]. The magnetic properties of  $\text{LaMn}_{0.5}\text{Ga}_{0.5}\text{O}_3$  are close to those of a purely ferromagnetic state with a Curie temperature  $T_C = 65$  K [8–10]. Goodenough [11, 12] first interpreted the ferromagnetism in this system as dynamic coupling of the filling of  $e_g$  orbitals with lattice vibrations, i.e., as “vibrational” superexchange. However, neutron diffraction studies of the  $\text{LaMn}_{1-x}\text{Ga}_x\text{O}_3$  system did not reveal an obvious structural heterogeneity [8]. Therefore, orbital ordering was assumed to be homogeneous throughout a crystal up to  $x = 0.5$ , and the magnetic structure was calculated in terms of a homogeneous model of canted magnetic sublattices [8]. To combine orbital ordering and ferromagnetism, the authors of [10] assumed that static orbital ordering can result in homogeneous ferromagnetic ordering by mixing the  $d_{z^2}$ - and  $d_{x^2-y^2}$ -orbitals. However, the orbital order–disorder transition is a first-order phase transition and proceeds through a two-phase state [12]. Moreover, double exchange is insignificant in  $\text{LaMn}_{1-x}\text{Ga}_x\text{O}_3$  and cannot cause a noncollinear magnetic structure. It is important to note that orbitally disordered  $\text{LaMn}_{0.4}\text{Ga}_{0.6}\text{O}_3$  is characterized by stronger positive exchange interactions as compared to  $\text{LaMn}_{0.5}\text{Ga}_{0.5}\text{O}_3$ , where orbital ordering is assumed [8]. Note that, according to dynamic magnetic sus-

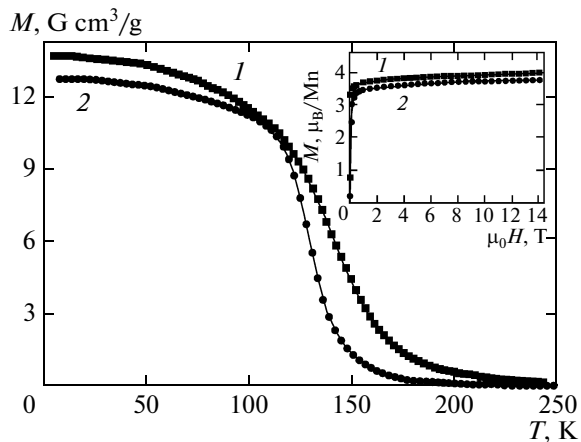


**Fig. 1.** Temperature dependences of the magnetizations of (1)  $\text{La}_{0.7}\text{Sr}_{0.3}\text{Mn}_{0.85}\text{Nb}_{0.15}\text{O}_3$  and (2)  $\text{La}_{0.7}\text{Sr}_{0.3}\text{Mn}_{0.85}\text{Nb}_{0.1}\text{Mg}_{0.05}\text{O}_3$  samples measured in an external magnetic field of 0.01 T. (inset) Field dependences of the magnetizations of these samples measured at  $T = 5$  K.

ceptibility measurements,  $\text{LaMn}_{0.5}\text{Ga}_{0.5}\text{O}_3$  contains antiferromagnetic clusters in a ferromagnetic matrix [14].

Farrell and Gehring [15] assumed that the substitution of gallium ions for manganese ions can transform the  $d_z^2$  orbitals into the  $d_{x^2-y^2}$  orbitals of neighboring manganese ions, which results in the formation of a ferromagnetic cluster around gallium ions. The later investigations of the local structure in the  $\text{LaMn}_{1-x}\text{Ga}_x\text{O}_3$  system did not reveal structural distortions of  $\text{MnO}_6$  octahedra in compositions at  $x > 0.5$  [16, 17]. Nevertheless, the Weiss constant of the composition with  $x = 0.6$  is higher than the composition with  $x = 0.5$  [8]. This finding indicates stronger ferromagnetic interactions in undistorted compositions, which is in conflict with the hypothesis of a transformation of the type of orbital ordering that was advanced in [15]. Structural studies of the  $\text{La}_{1-x}\text{Tb}_x\text{Mn}_{0.5}\text{Sc}_{0.5}\text{O}_3$  system showed that the structural distortions of  $\text{MnO}_6$  octahedra do not change up to  $x = 0.5$  [18]. In this case, however, the ferromagnetic state fully decomposes because of the enhancement of the role of antiferromagnetic interactions. This is caused by a decrease in the angle of the Mn–O–Mn bond, which controls the hybridization of the  $e_g$  orbitals of manganese and the  $2p$  orbitals of oxygen, i.e., covalence.

A dielectric ferromagnetic state was also detected in the  $\text{La}_{0.7}\text{Sr}_{0.3}\text{Mn}_{0.85}\text{Nb}_{0.15}\text{O}_3$  manganite, which has no manganese ions with different valences [19]. To reveal the nature of the ferromagnetic ordering in this manganite, we performed a neutron diffraction investigation of the crystal and magnetic structures of  $\text{La}_{0.7}\text{Sr}_{0.3}\text{Mn}_{0.85}\text{Nb}_{0.15-x}\text{Mg}_x\text{O}_3$  solid solutions at low temperatures. When  $\text{Mg}^{2+}$  ions substitute for  $\text{Nb}^{5+}$

ions, some manganese ions pass into the tetravalent state and an optimum doping regime formally appears. In this case, we expected an increase in the ferromagnetic properties due to double exchange. However, the ferromagnetism was found to weaken with increasing content of tetravalent manganese ions.

## 2. EXPERIMENTAL

Polycrystalline samples  $\text{La}_{0.7}\text{Sr}_{0.3}\text{Mn}_{0.85}\text{Nb}_{0.15-x}\text{Mg}_x\text{O}_3$  ( $x = 0, 0.05$ ) and  $\text{La}_{0.7}\text{Sr}_{0.3}\text{Mn}_{0.85}\text{Nb}_{0.15}\text{O}_3$  were prepared using solid-phase reactions according to a standard ceramic technology. Initial high-purity reagents  $\text{La}_2\text{O}_3$ ,  $\text{Mn}_2\text{O}_3$ ,  $\text{Nb}_2\text{O}_5$ ,  $\text{MgO}$ ,  $\text{SrCO}_3$ , and  $\text{CaCO}_3$  were taken in the stoichiometric ratio and thoroughly mixed (300 rpm, 30 min) in a PM-100 (RETSCH) planetary ball mill.  $\text{La}_2\text{O}_3$  was preliminarily annealed at a temperature of  $1100^\circ\text{C}$  to remove moisture. The samples were synthesized in the following two stages. The samples were first calcined at  $1400^\circ\text{C}$  for 5 h, and the final synthesis was performed in air at  $1500$ – $1550^\circ\text{C}$  for 7 h. The samples were then cooled at a rate of 300 K/h to a temperature of  $300^\circ\text{C}$ . Neutron diffraction studies were carried out on a high-resolution D2B (ILL, Grenoble, France) diffractometer. Crystal and magnetic structures were refined by the Rietveld method using the FullPROF software package. Magnetic measurements were performed on a device intended for measuring physical properties (Cryogenic Ltd.).

## 3. RESULTS AND DISCUSSION

The inset in Fig. 1 shows the field dependences of the magnetization of  $\text{La}_{0.7}\text{Sr}_{0.3}\text{Mn}_{0.85}\text{Nb}_{0.15}\text{O}_3$  and  $\text{La}_{0.7}\text{Sr}_{0.3}\text{Mn}_{0.85}\text{Nb}_{0.1}\text{Mg}_{0.05}\text{O}_3$  measured at  $T = 5$  K. The  $\text{La}_{0.7}\text{Sr}_{0.3}\text{Mn}_{0.85}\text{Nb}_{0.1}\text{Mg}_{0.05}\text{O}_3$  composition has about 20%  $\text{Mn}^{4+}$  ions; i.e., it is in a doping regime close to the optimum doping. It is seen that the spontaneous magnetic moment per manganese ion for the sample without magnesium ions exceeds  $3\mu_B$ . The coercive force is very low, which indicates a weak magnetic anisotropy. The appearance of manganese ions of different valences leads to an insignificant decrease in the spontaneous magnetization. The temperature dependences of the magnetization measured in a low external magnetic field also point to a certain decrease in the Curie temperature of the sample doped with tetravalent manganese ions (Fig. 1). Figure 2 shows the temperature and field dependences of the magnetization of the  $\text{La}_{0.7}\text{Ca}_{0.3}\text{Mn}_{0.85}\text{Nb}_{0.15}\text{O}_3$  sample. As  $\text{La}_{0.7}\text{Sr}_{0.3}\text{Mn}_{0.85}\text{Nb}_{0.15}\text{O}_3$ , this sample also has no manganese ions with different valences. The Curie temperature and the spontaneous magnetization are seen to decrease noticeably as compared to the  $\text{La}_{0.7}\text{Sr}_{0.3}\text{Mn}_{0.85}\text{Nb}_{0.15}\text{O}_3$  sample.

The neutron diffraction studies of the  $\text{La}_{0.7}\text{Sr}_{0.3}\text{Mn}_{0.85}\text{Nb}_{0.15-x}\text{Mg}_x\text{O}_3$  samples demonstrate that they have a rhombohedral structure (space group

$R\bar{3}c$ ) at room temperature. However, as the temperature decreases, a structural phase transition into the orthorhombic phase (space group  $Pnma$ ) occurs in the samples. This structural transition is not related to magnetic ordering, since it takes place well above the Curie temperature, near  $T = 250$  K. Figure 3 shows the calculated and refined neutron diffraction patterns of the  $\text{La}_{0.7}\text{Sr}_{0.3}\text{Mn}_{0.85}\text{Nb}_{0.15}\text{O}_3$  sample at  $T = 10$  K. The experimental and calculated patterns are seen to agree well with each other. The refinement of the populations of various crystal structure sites showed that the samples had stoichiometric cation and oxygen composition. The bond lengths between manganese and oxygen ions (Mn–O) in the orthorhombic phase differ insignificantly from each other, as in orbitally disordered orthorhombic  $\text{La}_{0.67}\text{Ca}_{0.33}\text{MnO}_3$ , which exhibits colossal magnetoresistance near the Curie point (table) [20]. The substitution of magnesium ions for niobium ions led to a decrease in the unit cell volume. However, the ionic radius of  $\text{Mg}^{2+}$  is larger than the ionic radius of  $\text{Nb}^{5+}$ ; therefore, the decrease in the unit cell volume is related to the formation of  $\text{Mn}^{4+}$  ions, the ionic radius of which is significantly smaller than that of  $\text{Mn}^{3+}$ . The refined magnetic moment per manganese ion is slightly higher in the sample without magnesium ions, which corresponds to magnetic measurements (table).

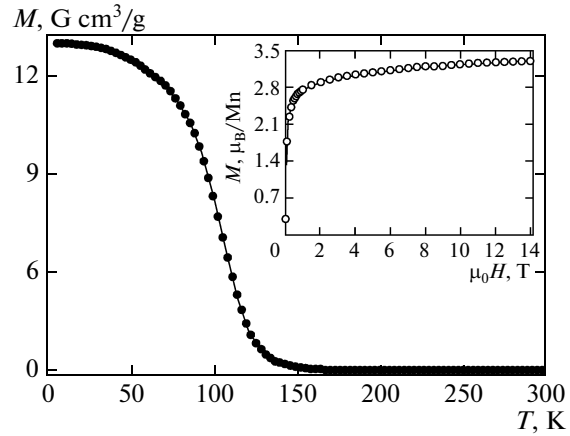


**Fig. 2.** Temperature dependence of the magnetization of an  $\text{La}_{0.7}\text{Ca}_{0.3}\text{Mn}_{0.85}\text{Nb}_{0.15}\text{O}_3$  sample measured in an external magnetic field of 0.01 T. (inset) Field dependence of the magnetization of this sample measured at  $T = 5$  K.

As follows from the calculation of the structure parameters, the orthorhombic lattice distortions do not result from cooperative orbital ordering. Both samples at low temperatures have approximately the same ratio of the lattice parameters, which is characteristic of the orbitally disordered phase. According to [8, 12, 15], cooperative orbital ordering should result

Crystalline and magnetic structure parameters refined by the Rietveld method for  $\text{La}_{0.7}\text{Sr}_{0.3}\text{Mn}_{0.85}\text{Nb}_{0.15}\text{O}_3$  and  $\text{La}_{0.7}\text{Sr}_{0.3}\text{Mn}_{0.85}\text{Nb}_{0.1}\text{Mg}_{0.05}\text{O}_3$  samples

Sample	$\text{La}_{0.7}\text{Sr}_{0.3}\text{Mn}_{0.85}\text{Nb}_{0.15}\text{O}_3$	$\text{La}_{0.7}\text{Sr}_{0.3}\text{Mn}_{0.85}\text{Nb}_{0.1}\text{Mg}_{0.05}\text{O}_3$
Temperature	10 K	5 K
Space group	$Pnma$	$Pnma$
Unit cell parameters		
$a$ , Å	5.521(1)	5.512(3)
$b$ , Å	7.810(2)	7.800(2)
$c$ , Å	5.557(7)	5.549(1)
Atom coordinates		
La/Sr	0.509(1), 0.25, 0.00001	0.513(1), 0.25, 0.002(1)
O(1)	−0.008(2), 0.25, −0.059(7)	−0.004(9), 0.25, −0.061(5)
O(2)	0.258(1), 0.031(2), 0.238(6)	0.265(6), 0.031(1), 0.233(9)
Bond lengths		
Mn–O(1), Å	1.981(1)	1.980(1)
Mn–O(2), Å	1.961(7)	1.971(2)
Mn–O(2), Å	1.988(3)	1.977(5)
Magnetic moment of Mn		
$\mu_z$ , $\mu_B$	3.1	3.0
Reliability factors		
$R_p/R_{wp}$ , %	5.08/6.58	3.53/5.09
$R_{\text{Bragg}}$ , %	6.07	3.65
Magnetic $R$ factor	11.5	5.61

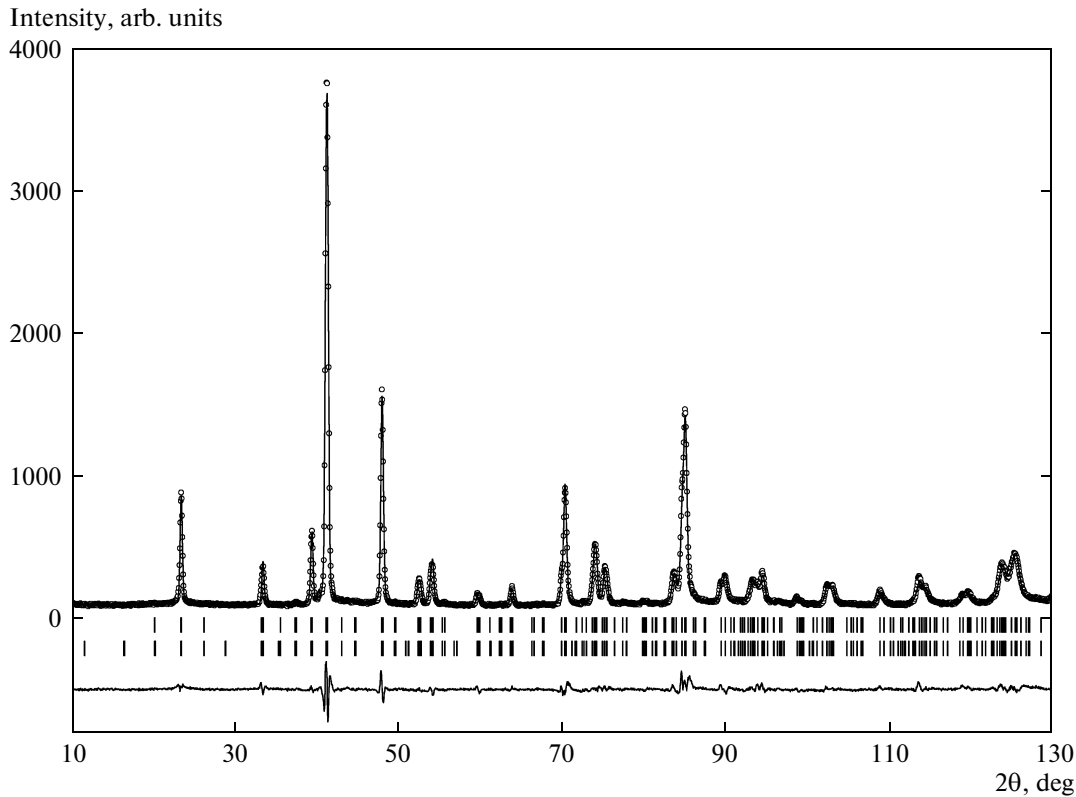


**Fig. 3.** (points) Measured and (solid curve) calculated neutron diffraction patterns of an  $\text{La}_{0.7}\text{Sr}_{0.3}\text{Mn}_{0.85}\text{Nb}_{0.15}\text{O}_3$  sample ( $T = 10$  K). Vertical bars indicate Bragg reflections: the upper row belongs to a crystalline phase, and the lower row, to a magnetic phase. The lower curve corresponds to the difference between the measured and calculated values.

in the relation  $b/\sqrt{2} < c < a$  between the unit cell parameters, whereas we detected the relation  $c > a \approx b/\sqrt{2}$ , which is characteristic of non-Jahn–Teller ferrite and chromite systems with a perovskite structure. However, based on our data, we cannot exclude local static Jahn–Teller distortions. Therefore, the ferromagnetism of the samples under study cannot be caused by cooperative orbital ordering or double exchange. According to the Goodenough–Kanamori rules, the sign of the  $180^\circ$  superexchange interaction between  $\text{Mn}(e_g)\text{—O—Mn}(e_g)$  for the  $\text{Mn}^{3+}$  ion is not determined in the case of no orbital ordering [9]. This means that the antiferromagnetic part of the exchange is equal to the ferromagnetic part. However, this is true of only the case of a purely ionic bond with integer cation and anion valences. In the case of a covalent component of the chemical bond, the  $e_g$  orbitals of manganese and the  $2p$  orbitals of oxygen undergo hybridization. This means that  $e_g$  electrons are located at oxygen for some time and the formal population of the  $e_g$  orbitals of manganese decreases, favoring an increase in the ferromagnetic fraction of superexchange. In the ion model, a similar effect occurs when divalent alkaline-earth ions substitute for some trivalent lanthanum ions. In this case, tetravalent manganese ions appear.

Covalence leads to a mixed valence of ions due to averaging of the electron density on a certain time scale. A decrease in the covalent component of the bond causes a decrease in the ferromagnetic component irrespective of the  $\text{Mn}^{3+}/\text{Mn}^{4+}$  ratio. For example, the Curie temperature of weakly distorted  $\text{La}_{0.7}\text{Sr}_{0.3}\text{MnO}_3$  is 380 K, whereas the Curie temperature of  $\text{La}_{0.7}\text{Ca}_{0.3}\text{MnO}_3$  is 250 K. The distortions in the latter composition are substantially larger. A similar picture is observed for compositions free of  $\text{Mn}^{4+}$  ions (Figs. 1, 2). On the other hand, structural disordering can weaken the covalence because of local variations of the Mn–O–Mn bond angle. This angle controls the hybridization of the orbitals of manganese and oxygen. This effect is most likely to weaken the ferromagnetism in the sample with magnesium ions. When studying the structure of the  $\text{La}_{1-x}\text{Tb}_x\text{Mn}_{0.5}\text{Sc}_{0.5}\text{O}_3$  system, the authors of [18] showed that the structural distortions of  $\text{MnO}_6$  octahedra did not change up to  $x = 0.5$ . However, the ferromagnetic state here fully decomposes (spin glass) because of increasing the role of antiferromagnetic interactions. This process is caused by a decrease in the Mn–O–Mn bond angle, which controls the hybridization of the  $e_g$  orbitals of manganese and the  $2p$  orbitals of oxygen, i.e., the covalence.

According to spectroscopic studies, the density of states near the Fermi surface in metallic manganites is very low, which is explained by the formation of a pseudogap because of strong correlation effects [21]. This finding agrees with a theoretical consideration, which demonstrates that most  $e_g$  electrons in manganites in the metallic state are localized [22]. In this case, ferromagnetism can be caused by the positive superexchange interactions that are related to the virtual excitation of  $e_g$  electrons to the orbitals of neighboring  $Mn^{3+}$  and  $Mn^{4+}$  ions. This assumption agrees well with the magnetic phase diagrams of half-doped manganites. In these manganites, the antiferromagnetic and ferromagnetic parts of the superexchange interactions are very close to each other, and small changes of the parameters result in a transition from one to another magnetic state and in colossal magnetoresistance [23]. The formation of an antiferromagnetic metallic  $A$ -type state with a high Néel temperature also indicates a localized character of most  $e_g$  electrons and a weak role of charge carriers in exchange interactions [23]. The antiferromagnetism of more than half-doped manganites is clearly understood in terms of the superexchange interaction model. In this case, the antiferromagnetic contribution of  $t_{2g}$  electrons dominates over the contribution of  $e_g$  electrons, since their number decreases with increasing alkaline-earth metal concentration. Under optimum doping, the lattice distortions are minimal and the antiferromagnetic interactions are weak. However, the orthorhombic lattice distortions in  $La_{0.7}Ca_{0.3}MnO_3$  lead to the competition of exchange interactions and colossal magnetoresistance near  $T_C$ . In this case, antiferromagnetic clusters were revealed in the paramagnetic region above  $T_C$  [24]. The competition between more covalent ferromagnetic and less covalent (more structurally distorted) antiferromagnetic states also causes colossal magnetoresistance in cobaltites [25].

Ferromagnetic ordering is most likely not to be compatible with the orbital ordering of the  $LaMnO_3$  type. Indeed, the neutron diffraction studies of the  $LaMn_{1-x}Ga_xO_3$  system [8] point to the presence of two magnetic phases, since the Curie and Néel temperatures are different in some compositions. The magnetic susceptibility of  $LaMn_{0.5}Ga_{0.5}O_3$  increases sharply at a moderate pressure [9]. This finding suggests that this composition has antiferromagnetic clusters at a normal pressure, which transform into a ferromagnetic state under pressure or in an external magnetic field. The two-phase structure can be masked by stress relaxation through a coherent interface. Neutron diffraction studies revealed a magnetic two-phase state in weakly doped  $La_{1-x}Sr_xMnO_3$  ( $x = 0.125$ ) single crystals [7]. The detected antiferromagnetic  $A$ -type phase is most likely to be caused by local orbital ordering, which is similar to that detected in the initial  $LaMnO_3$  compound (which is also a  $A$ -type antiferromagnet).

In conclusion, we note that our studies and analysis of experimental data demonstrate that the ferromagnetism of manganites is caused by superexchange interactions, which are most likely to be stronger than double exchange. In terms of this model, this ferromagnetism is related to virtual excitations of  $e_g$  electrons and their passage to the vacant orbitals of neighboring  $Mn^{3+}$  and  $Mn^{4+}$  ions, which are facilitated in the presence of a sufficiently strong covalent bond. Structural lattice distortions and orbital ordering weaken the covalent component of the chemical bond, enhance the antiferromagnetic part of exchange interactions, and favor deep carrier localization. The magnetoresistance is caused by the fact that the positive and negative parts of the superexchange interactions can be close to each other in magnitude and a magnetic field induces a ferromagnetic conducting state.

### ACKNOWLEDGMENTS

This work was supported by the Belarussian Foundation for Basic Research, project no. F12SO-026.

### REFERENCES

1. C. Zener, Phys. Rev. **82**, 403 (1951).
2. C. Şen, G. Alvarez, and E. Dagotto, Phys. Rev. Lett. **98**, 127202 (2007).
3. P.-G. de Gennes, Phys. Rev. **118**, 141 (1960).
4. G. Allodi, R. De Renzi, G. Guidi, F. Licci, and M. W. Pieper, Phys. Rev. B: Condens. Matter **56**, 6036 (1997).
5. K. Kumagai, A. Iwai, Y. Tomioka, H. Kuwahara, Y. Tokura, and A. Yakubovskii, Phys. Rev. B: Condens. Matter **59**, 97 (1999).
6. M. Hennion and F. Moussa, New J. Phys. **7**, 84 (2005).
7. H.-F. Li, Y. Su, Y. G. Xiao, J. Persson, P. Meuffels, and Th. Brückel, Eur. Phys. J. B **67**, 149 (2009).
8. J. Blasco, J. García, J. Campo, C. Sánchez, and G. Subías, Phys. Rev. B: Condens. Matter **66**, 174431 (2002).
9. J.-S. Zhou, Y. Uwatoko, K. Matsubayashi, and J. B. Goodenough, Phys. Rev. B: Condens. Matter **78**, 220402(R) (2008).
10. J.-S. Zhou and J. B. Goodenough, Phys. Rev. B: Condens. Matter **77**, 172409 (2008).
11. J.-S. Zhou, H. Q. Yin, and J. B. Goodenough, Phys. Rev. B: Condens. Matter **63**, 184423 (2001).
12. J.-S. Zhou and J. B. Goodenough, Phys. Rev. B: Condens. Matter **60**, R15002 (1999).
13. I. O. Troyanchuk, D. D. Khalyavin, and H. Szymczak, Mat. Res. Bull. **32**, 1637 (1997).
14. D. Rinaldi, R. Caciuffo, J. J. Neumeier, D. Fiorani, and S. B. Oseroff, J. Magn. Magn. Mater. **272–276**, E571 (2004).
15. J. Farrell and G. A. Gehring, New J. Phys. **6**, 168 (2004).
16. M. C. Sánchez, G. Subías, J. García, and J. Blasco, Phys. Scr. **2005**, 641 (2005).

17. M. C. Sánchez, J. García, G. Subías, and J. Blasco, *Phys. Rev. B: Condens. Matter* **73**, 094416 (2006).
18. J. Blasco, V. Cuartero, J. García, and J. A. Rodríguez-Velamazán, *J. Phys.: Condens. Matter* **24**, 076006 (2012).
19. I. O. Troyanchuk, M. V. Bushinsky, H. Szymczak, K. Bärner, and A. Maignan, *Eur. Phys. J. B* **28**, 75 (2002).
20. Q. Huang, A. Santoro, J. W. Lynn, R. W. Erwin, J. A. Borchers, J. L. Peng, K. Ghosh, and R. L. Greene, *Phys. Rev. B: Condens. Matter* **58**, 2684 (1998).
21. T. Saitoh, D. S. Dessau, Y. Moritomo, T. Kimura, Y. Tokura, and N. Hamada, *Phys. Rev. B: Condens. Matter* **62**, 1039 (2000).
22. T. V. Ramakrishnan, H. R. Krishnamurthy, S. R. Hassan, and G. Venkateswara Pai, *Phys. Rev. Lett.* **92**, 157203 (2004).
23. Y. Tokura, *Rep. Prog. Phys.* **69**, 797 (2006).
24. D. N. Argyriou, J. W. Lynn, R. Osborn, B. Campbell, J. F. Mitchell, U. Ruett, H. N. Bordallo, A. Wildes, and C. D. Ling, *Phys. Rev. Lett.* **89**, 036401 (2002).
25. I. O. Troyanchuk, M. V. Bushinsky, and L. S. Lobanovsky, *J. Appl. Phys.* **114**, 213910 (2013).

*Translated by K. Shakhlevich*